

High-Field Transport in an Electron-Hole Plasma: Transition from Ballistic to Drift Motion

P. Bowlan,¹ W. Kuehn,¹ K. Reimann,¹ M. Woerner,¹ T. Elsaesser,¹ R. Hey,² and C. Flytzanis³

¹*Max-Born-Institut für Nichtlineare Optik und Kurzzeitspektroskopie, 12489 Berlin, Germany*

²*Paul-Drude-Institut für Festkörperelektronik, 10117 Berlin, Germany*

³*Laboratoire Pierre Aigrain, École Normale Supérieure, 75231 Paris, France*

(Received 1 July 2011; published 15 December 2011)

The time evolution of high-field carrier transport in bulk GaAs is studied with intense femtosecond THz pulses. While ballistic transport of electrons occurs in an *n*-type sample, a transition from ballistic to driftlike motion is observed in an electron-hole plasma. This onset of friction is due to the holes, which are heated by THz absorption. Theoretical calculations, which reproduce the data quantitatively, show that both electron-hole scattering and local-field effects in the electron-hole plasma are essential for the time-dependent friction.

DOI: [10.1103/PhysRevLett.107.256602](https://doi.org/10.1103/PhysRevLett.107.256602)

PACS numbers: 72.20.Ht, 72.80.Ey, 78.47.J–

In the absence of scattering, an electron in a crystal travels ballistically driven by an external electric field E . In momentum or k space, the electron follows the dispersion of the conduction band at a rate dk/dt proportional to the driving field E . As a result, the electron performs coherent Bloch oscillations in both real and momentum space. Bloch oscillations have been observed in semiconductor superlattices, atomic ensembles in optical lattices, and other tailored systems [1,2]. Recently, partial Bloch oscillations covering half the first Brillouin zone of bulk GaAs have been induced by driving electrons with high electric fields with frequencies in the THz range [3].

In most cases, however, electric charge transport in metals and semiconductors occurs under conditions where scattering of electrons with the lattice randomizes the electron motion, limiting the velocity. Eventually, such friction results in driftlike transport, in which the electron velocity is proportional to the driving electric field. Microscopic interactions such as electron-phonon scattering, electron-impurity scattering, and scattering from imperfect interfaces in low-dimensional systems result in scattering times down to the sub-100 fs time range, destroying transport coherences very efficiently. In the most conventional approach, this transport regime is described by the semiclassical Boltzmann transport equation with scattering rates calculated from perturbation theory [4,5].

So far, the transition from coherent ballistic to incoherent driftlike transport has not been explored in much detail. This transition regime is highly relevant for understanding the onset of friction, which is connected with quantum coherences and their damping by interactions among carriers and with the lattice. Such phenomena are important for understanding basic physical properties of coherent charge transport in solids and for solid state devices working at high bias fields and/or frequencies. High-field transport studies with femtosecond time resolution can give specific insight into ultrafast transport dynamics. Clear signatures of coherent ballistic transport of electrons [3]

and quantum kinetic features of polaron transport [6] have been revealed in femtosecond THz studies with (single-component) electron plasmas in *n*-type GaAs. On the other hand, drift velocities of a photoexcited electron-hole plasma in electrically biased bulk GaAs and InP have been derived from the time-resolved THz emission of the accelerated carriers [7–9]. The velocity overshoot during the first 500 fs has been attributed to electrons only, while the drift current at later times has been assigned to a superposition of electron and hole currents. The role of electron-hole interactions for the initial decoherence and the buildup of frictional forces has not been addressed and is not understood so far.

In this Letter, we present a study of high-field charge transport in an electron-hole plasma driven by ultrashort THz transients. A systematic variation of experimental conditions gives clear insight into the transition from ballistic to driftlike electron transport. While the hole current is much smaller than the electron current, the presence of holes has a strong impact on electron transport by introducing a friction force that builds up on a time scale of the order of 1 ps. This friction originates from the heating of the hole distribution by the THz driving field and the resulting enhanced electron-hole scattering. We describe our measurements with a theoretical model for the transient dielectric function of the electron-hole system and show that the time-dependent screening of the external field by the carrier plasma leads to pronounced local-field effects. The model correctly describes the transition from ballistic to drift transport and the influence of holes on electron motion. Beyond semiconductor physics our new insight into friction caused by interactions among carriers is relevant for other transport phenomena such as electrons in ionic plasmas and ions in quantum gases [10–12].

In our experiments, the carriers in the sample are accelerated by an external THz field transient with a maximum amplitude of 50 kV/cm. The field radiated by the carriers is detected in amplitude and phase by electro-optic sampling.

The setup is the same as the setup shown in Fig. 2 of [13], except that for photoexcitation an additional near-infrared beam is incident on the sample. Using a sample with a thickness d much less than the THz wavelength of $150 \mu\text{m}$, the emitted electric field $E_{\text{em}}(t)$ is proportional to the current $j(t)$ (see [13,14]):

$$j(t) = -env_e(t) + j_h^{\text{intra}}(t) + j_h^{\text{inter}}(t) = -2E_{\text{em}}(t)/(Z_0d), \quad (1)$$

where e is the elementary charge, n the electron density, $v_e(t)$ their velocity, and Z_0 the impedance of free space. There are two contributions from holes, the intraband current $j_h^{\text{intra}} = e(p_{hh}v_{hh} + p_{lh}v_{lh})$ of heavy and light holes and the current j_h^{inter} from the interband hh - lh polarization. Because of radiative coupling [15,16], the driving field, $E_{\text{dr}}(t)$, is not the incident THz field, but the THz field transmitted through the sample. Since both the current and the driving field are measured as a function of time, we can easily distinguish between drift transport [$j(t) \propto E_{\text{dr}}(t)$] and ballistic transport. In the present experiments, the field amplitude is low enough to limit ballistic electron motion to the parabolic Γ valley so that $m\vec{v}_e = \hbar\vec{k}$ (m : constant effective electron mass, \vec{k} electron wave vector) and $j(t) \propto \int_{-\infty}^t E_{\text{dr}}(t')dt'$.

In the samples, the carriers are present because of doping and/or are generated by interband photoexcitation with ≈ 100 fs pulses. Our samples grown by molecular beam epitaxy consist each of a 500 nm thin GaAs layer [17] clad between two undoped 300 nm $\text{Al}_{0.4}\text{Ga}_{0.6}\text{As}$ barriers. The GaAs layer is either undoped, n type ($N_D = 2 \times 10^{16} \text{ cm}^{-3}$), or p type ($N_A = 3 \times 10^{16} \text{ cm}^{-3}$). Because we work at $T_L = 300$ K, the carrier density from doping is equal to the dopant density (for electrons $n = N_D$, for holes $p = N_A$).

To measure the current from electrons only, or from holes only, we use the n - and p -type samples and measure THz transients with and without the sample. The difference between these two transients is the electric field emitted by the carriers present by doping [Eq. (1)]. Additionally, by photoexcitation we can introduce an electron-hole plasma. To measure the current from the electron-hole plasma the THz field transmitted through the sample is measured with and without the photoexcitation pulse. The difference between these two field transients is the current from the electron-hole plasma.

First we compare the transport of holes only (p -type sample), of electrons only (n -type sample), and of electrons and holes together (Fig. 1). For the last case we photoexcite the undoped sample to generate electrons and holes with densities of $n = p \approx 2 \times 10^{16} \text{ cm}^{-3}$. The excitation is resonant to the GaAs band gap ($\lambda_{\text{exc}} = 885 \text{ nm}$). After photoexcitation, the THz pulse is delayed by $\tau = 1.5$ ps to ensure that the carriers have thermalized and cooled to the lattice temperature [18,19].

The results in Fig. 1 show that transport in the three cases is quite different. In the p -type sample [Fig. 1(a)], the

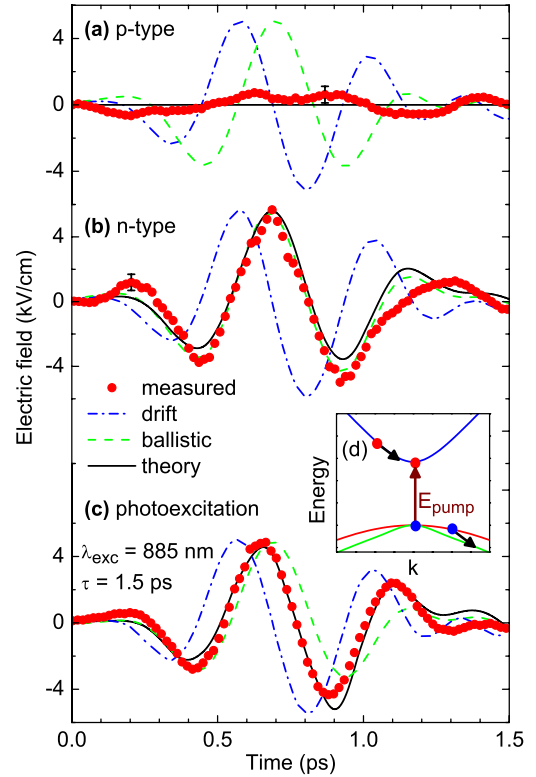


FIG. 1 (color online). Measured emitted fields (proportional to the current, dots) from (a) holes only, (b) electrons only, and (c) from an electron-hole plasma. The measured data are compared with two limiting cases: Perfect drift transport (dash-dotted line) and perfect ballistic transport (dashed line). The solid lines give the results of our model. The experimental errors are shown by error bars in (a) and (b) and by the symbol size in (c) and in Fig. 2. (d) Band structure of GaAs near $k = 0$.

amplitude of the emitted field is 5 times smaller than for the n -type sample [Fig. 1(b)] and of the same magnitude as the error bars. The n -type sample shows perfect ballistic electron motion (cf. Ref. [3]), representing the absence of scattering. In contrast, the field emitted by the photoexcited carriers [Fig. 1(c)] is ballistic in the beginning of the pulse, but gradually becomes more driftlike at later times. Considering that the current in the p -type sample was very small, we conclude that the current in the electron-hole plasma comes predominantly from electrons. Since it differs from the current in the n -type sample, electron-hole interactions are clearly affecting the electron transport. These interactions introduce a time-dependent dissipation over the duration of the THz pulse without decreasing the field amplitude.

Additionally, we compared the current of photoexcited carriers in the three different samples as shown in Fig. 2. For this experiment we used an excitation wavelength of $\lambda_{\text{exc}} = 830 \text{ nm}$ to ensure that the absorption (and thus the excited density) was the same in the three samples [20]. Here the THz pulse was delayed by $\tau = 15$ ps. All other experimental parameters, such as photoexcited density and

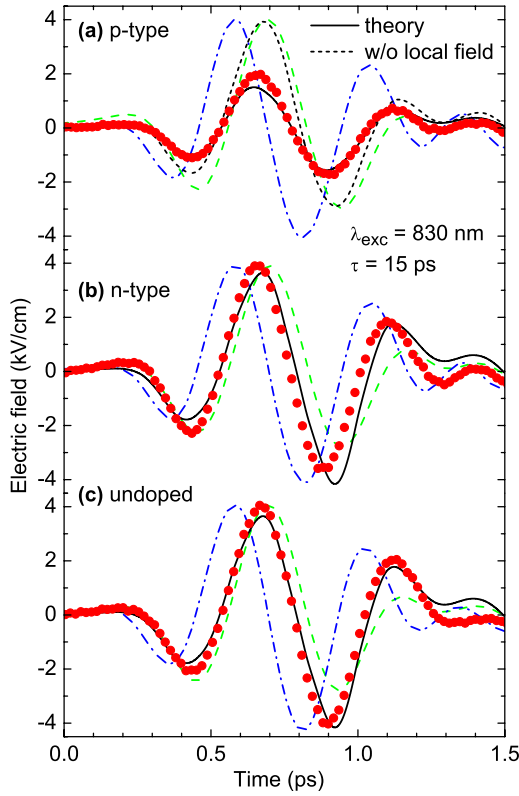


FIG. 2 (color online). Field emitted (dots) by photoinjected carriers in (a) a *p*-type sample, (b) an *n*-type sample, and (c) an undoped sample. Again, the two limiting cases of ballistic transport (dashed line) and drift transport (dash-dotted line), and the results of our model (solid line) are shown. In (a), the theory without local-field correction is also shown (dotted line).

field strength, were the same as in Fig. 1. The results for the undoped sample [Figs. 1(c) and 2(c)] are the same for the two excitation wavelengths, which confirms that the electron distributions after thermalization and cooling were the same. While all three samples show a gradual transition from ballistic to drift transport, the amplitude of the current varies. In particular, in the *p*-type sample, when additional holes are present, the current is 2 times smaller.

In electron-hole plasmas, there are two mechanisms of light-matter interaction: (i) the acceleration of carriers, and (ii) the absorption of the THz field via intervalence band transitions of holes. In our experiments, the small hole currents are within the noise limit [Fig. 1(a)]. The intra-band current $j_h^{\text{intra}}(t)$ of heavy holes, the predominant hole species, is low because of the large effective mass. Furthermore, it is partly compensated by the interband current $j_h^{\text{inter}}(t)$ of opposite direction. Therefore we neglect the hole currents in the following. The electron ensemble is characterized by an average wave vector $k \neq 0$ and a width $\sqrt{\Delta k^2}$. In a parabolic band, k is proportional to the current and Δk^2 determines its dynamics. In the ballistic limit [Fig. 1(b)] $k \gg \sqrt{\Delta k^2}$. Carrier thermalization and intervalence band scattering of holes occur on a sub-100 fs time

scale [21] and, thus, it is justified to assume a common carrier temperature T_{eh} to describe Δk^2 . Interaction of electrons with holes results in a gradual increase of Δk^2 , i.e., an increase of T_{eh} , causing a transition to driftlike transport.

The experimentally observed high-field transport is modeled theoretically by the frequency and wave-vector dependent dielectric function $\varepsilon(\omega, q)$, consisting [22–25] of the high-frequency background due to bound electrons (ε_∞), the lattice contribution [$\chi_L(\omega)$] and contributions from the free electrons and holes. Since both heavy-hole and light-hole bands are involved, inter-valence-band contributions to $\varepsilon(\omega, q)$ have to be included.

The change of the electron velocity with time is due to the force from the local electric field acting on the electron and to a friction force. This leads to:

$$\frac{dv_e}{dt} = -\frac{v_e}{\tau_m(v_e, p, T_{\text{eh}}, T_L)} - \frac{eE_{\text{loc}}(t, p, T_{\text{eh}})}{m}. \quad (2)$$

Instead of the friction force we use the momentum relaxation time τ_m . To determine the dependence of τ_m on v_e , p , T_{eh} , and T_L [19], we extended the concept of Eq. (57) of [26] to the more general loss function concept [23,24]. Furthermore, we included the finite size of the electron wave packet (the thermal de Broglie wavelength [3,27], $(\Delta x^2)^{-1} = 4\Delta k^2 = 4mk_B T_{\text{eh}}/\hbar$):

$$\tau_m^{-1} = \frac{e^2}{k^2 \varepsilon_0} \int_{-\infty}^{\infty} \int_{-\infty}^{\infty} \exp\left(\frac{-\hbar^2 q^2}{4mk_B T_{\text{eh}}}\right) \frac{\vec{q} \cdot \vec{k}}{q^2 |\varepsilon(\omega, q)|^2} \times \left\{ \frac{\text{Im}[\chi_L(\omega)]}{\exp(-\hbar\omega/k_B T_L) - 1} + \frac{\text{Im}[\chi_h(\omega, q, T_{\text{eh}})]}{\exp(-\hbar\omega/k_B T_{\text{eh}}) - 1} \right\} \times \delta\left(\frac{\hbar^2[(\vec{k} + \vec{q})^2 - k^2]}{2m} + \hbar\omega\right) d^3 \vec{q} d\omega. \quad (3)$$

This equation contains the hole susceptibility χ_h with contributions from both light and heavy holes but not the electron susceptibility, since electron-electron scattering alone cannot change the total momentum of the electron ensemble and, thus, cannot lead to friction.

The energy deposited in the sample via THz absorption heats the carrier system and yields a time-dependent carrier temperature $T_{\text{eh}}(t)$:

$$\frac{3}{2} k_B [T_{\text{eh}}(t) - T_L] = \frac{-en}{n+p} \int_{-\infty}^t v_e(t') E_{\text{dr}}(t') dt' - \frac{mv_e^2(t)}{2}. \quad (4)$$

$T_{\text{eh}}(t)$ is given by the total deposited energy minus the kinetic energy of the electrons undergoing transport. The total time-dependent deposited energy is shown in Fig. 3(a). The energy left in the carrier system after the end of the THz pulse is very small for the *n*- and *p*-type samples, pointing to small THz absorption and minor changes of T_{eh} , while carrier temperatures higher than 4000 K are found for the photoexcited samples. In

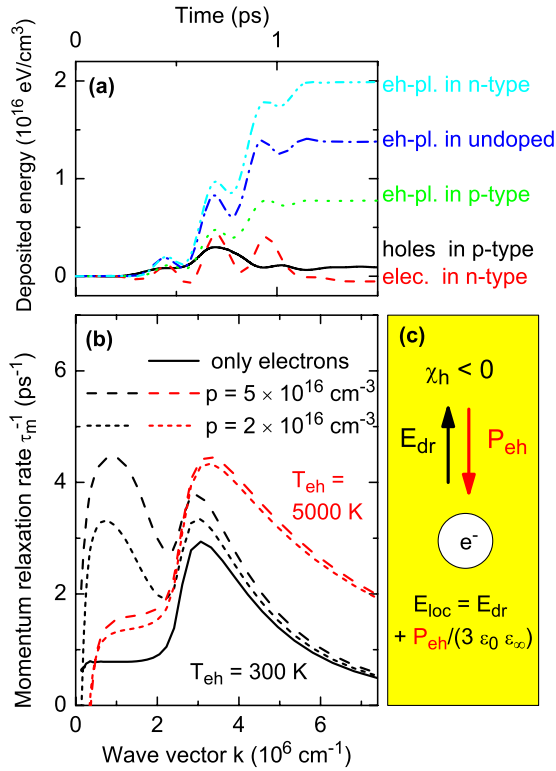


FIG. 3 (color online). (a) Measured deposited energy density $W(t) = \int_{-\infty}^t j(t')E_{dr}(t')dt'$. (b) Calculated momentum relaxation rates τ_m^{-1} of an electron in the Γ valley as a function of its wave vector k . Solid line: no holes, interaction only with LO phonons. Long and short dashed lines: interaction with both LO phonons and holes for hole densities p and carrier temperatures T_{eh} as indicated. (c) Schematic of the local-field correction to the driving field E_{dr} experienced by an electron embedded in an electron-hole plasma with the susceptibility $\chi_h(\omega_{THz}, q_h, T_{eh}) < 0$.

Fig. 3(b), the resulting friction is plotted as a function of the electron wave vector and compared to the friction for the initial $T_{eh} = 300$ K. The strong enhancement of friction results in the transition from ballistic to driftlike transport as shown in Figs. 1 and 2. For a quantitative comparison of theory and experiment, the influence of the holes on the local field experienced by an electron (and vice versa) has to be included:

$$E_{loc}(t, p, T_{eh}) = E_{dr}(t) \left[1 + \frac{\chi_h(\omega_{THz}, q_h, T_{eh})}{3\epsilon_0\epsilon_\infty} \right]. \quad (5)$$

The relevant wave vector q_h in Eq. (5) is determined by the average distance between holes, $q_h \approx p^{1/3}$. The local field [Eq. (5)] differs from the driving field by the Lorenz-Lorentz field [5,28–30]. As illustrated schematically in Fig. 3(c), the driving field E_{dr} creates a macroscopic polarization in the electron-hole plasma P_{eh} . The Lorenz-Lorentz field in a spherical cavity around an electron produces an additional contribution to the local field $E_{loc} = E_{dr} + P_{eh}/(3\epsilon_0\epsilon_\infty)$. Similar to the arguments given

above, the electron susceptibility does not screen the interaction of electrons with the driving field E_{dr} , since it cannot introduce a relative motion between electrons. At low carrier temperatures $T_{eh} \approx 300$ K, the hole susceptibility $\chi_h(\omega_{THz}, q_h, T_{eh})$ in Eq. (5) is negative for our ω_{THz} [22] and, thus, reduces the local field E_{loc} . As the plasma temperature increases, the screening power of the holes gets lost, resulting in a vanishing local-field correction for the interaction of electrons with the driving field.

Our theoretical calculations (solid lines in Figs. 1 and 2) reproduce the experimental results quantitatively. At the beginning of the THz pulse the carrier temperature is low, leading to low friction and thus to ballistic transport. During the THz pulse, if both holes and electrons are present, the carrier temperature increases because of heavy-hole–light-hole transitions and subsequent heating of electrons. The increase of carrier temperature increases the friction, so that the transport becomes more driftlike. Stronger friction would result in a decrease of current amplitude, but this is compensated by the decrease of the local-field correction for higher temperature (see dotted line in Fig. 2).

In conclusion, we studied ultrafast high-field transport of an electron-hole plasma using ultrashort THz pulses as the driving field. We find that the current in an electron-hole plasma is not equal to the sum of the currents in an n -type sample (only electrons) and a p -type sample (only holes). While the hole current is negligible compared to the electron current, the presence of holes leads to a transition of electron transport from ballistic to driftlike. This buildup of friction is caused by electron-hole interaction leading to local-field effects and a strong energy exchange.

- [1] J. Feldmann, K. Leo, J. Shah, D.A.B. Miller, J.E. Cunningham, T. Meier, G. von Plessen, A. Schulze, P. Thomas, and S. Schmitt-Rink, *Phys. Rev. B* **46**, 7252 (1992).
- [2] I. Bloch, *Nature (London)* **453**, 1016 (2008).
- [3] W. Kuehn, P. Gaal, K. Reimann, M. Woerner, T. Elsaesser, and R. Hey, *Phys. Rev. Lett.* **104**, 146602 (2010).
- [4] M. V. Fischetti, *IEEE Trans. Electron Devices* **38**, 634 (1991).
- [5] G. D. Mahan, *Many-Particle Physics* (Kluwer, New York, 2000), 3rd ed..
- [6] P. Gaal, W. Kuehn, K. Reimann, M. Woerner, T. Elsaesser, and R. Hey, *Nature (London)* **450**, 1210 (2007).
- [7] A. Leitenstorfer, S. Hunsche, J. Shah, M. C. Nuss, and W. H. Knox, *Phys. Rev. Lett.* **82**, 5140 (1999).
- [8] A. Leitenstorfer, S. Hunsche, J. Shah, M. C. Nuss, and W. H. Knox, *Phys. Rev. B* **61**, 16642 (2000).
- [9] M. Abe, S. Madhavi, Y. Shimada, Y. Otsuka, K. Hirakawa, and K. Tomizawa, *Appl. Phys. Lett.* **81**, 679 (2002).
- [10] P. K. Shukla and B. Eliasson, *Rev. Mod. Phys.* **83**, 885 (2011).
- [11] M. Bonitz, C. Henning, and D. Block, *Rep. Prog. Phys.* **73**, 066501 (2010).

- [12] U. Schneider, L. Hackermüller, S. Will, T. Best, I. Bloch, T.A. Costi, R.W. Helmes, D. Rasch, and A. Rosch, *Science* **322**, 1520 (2008).
- [13] W. Kuehn, P. Gaal, K. Reimann, M. Woerner, T. Elsaesser, and R. Hey, *Phys. Rev. B* **82**, 075204 (2010).
- [14] K. Reimann, *Rep. Prog. Phys.* **70**, 1597 (2007).
- [15] T. Stroucken, A. Knorr, P. Thomas, and S. W. Koch, *Phys. Rev. B* **53**, 2026 (1996).
- [16] T. Shih, K. Reimann, M. Woerner, T. Elsaesser, I. Waldmüller, A. Knorr, R. Hey, and K.H. Ploog, *Phys. Rev. B* **72**, 195338 (2005).
- [17] This thickness is large enough that confinement is negligible, but still small compared to the THz wavelength.
- [18] J. Shah, *Ultrafast Spectroscopy of Semiconductors and Semiconductor Nanostructures* (Springer, Berlin, 1999), 2nd ed..
- [19] For excitation resonant to the band gap and for the present excitation density, hot-phonon effects are negligible.
- [20] The band gap varies with doping, so that the absorption at 885 nm would be different for the three samples.
- [21] T. Elsaesser, J. Shah, L. Rota, and P. Lugli, *Phys. Rev. Lett.* **66**, 1757 (1991).
- [22] W. Bardyszewski, *Solid State Commun.* **57**, 873 (1986).
- [23] A.F.J. Levi and Y. Yafet, *Appl. Phys. Lett.* **51**, 42 (1987).
- [24] J.F. Young and P.J. Kelly, *Phys. Rev. B* **47**, 6316 (1993).
- [25] M. Woerner and T. Elsaesser, *Phys. Rev. B* **51**, 17490 (1995).
- [26] N. Janssen and W. Zwerger, *Phys. Rev. B* **52**, 9406 (1995).
- [27] F.M. Peeters and J.T. Devreese, *Phys. Rev. B* **31**, 4890 (1985).
- [28] O.F. Mossotti, *Mem. Matem. Sci. Fis. Nat. Soc. Ital. Sci.* **24**, 49 (1850).
- [29] H.A. Lorentz, *Wiedemanns Ann.* **9**, 641 (1880).
- [30] L. Lorenz, *Wiedemanns Ann.* **11**, 70 (1881).